

Supplement of Atmos. Chem. Phys., 20, 9915–9938, 2020  
<https://doi.org/10.5194/acp-20-9915-2020-supplement>  
© Author(s) 2020. This work is distributed under  
the Creative Commons Attribution 4.0 License.



*Supplement of*

## **Statistical regularization for trend detection: an integrated approach for detecting long-term trends from sparse tropospheric ozone profiles**

**Kai-Lan Chang et al.**

*Correspondence to:* Kai-Lan Chang ([kai-lan.chang@noaa.gov](mailto:kai-lan.chang@noaa.gov))

The copyright of individual parts of the supplement might differ from the CC BY 4.0 License.

## List of Tables

S-1	Percentage of (A) randomly generated and (B) fixed frequency sampled trends that fall outside of the 1- or 2- $\sigma$ intervals of the trend values that were derived from the full IAGOS data set. One thousand randomly generated trends were calculated on 15 pressure surfaces for each of a pre-determined scenario. Also shown are the associated mean absolute percentage error values. . . . .	2
S-2	Trends and 2-sigma variabilities [in units of ppb decade <sup>-1</sup> ] based on the separated fit and integrated fit methods, with a reference to different starting year, above Hilo, Hawaii and Trinidad Head (THD), California. . . . .	2

## List of Figures

S-1	A synthetic profile for the illustration of the issue of underfitting and overfitting. Data points are generated by adding random error to the function $x = \sin(y/100) \times (y/100)^2$ (black curve). The appropriate fit should closely follow the true process (red curve), while the underfit indicates that the result failed to represent the general pattern of the true process (blue curve), and the overfit indicates that the result is overly complicated and is influenced by the noise component (green curve). Note that these three fits are based on the same model specification, except that we adjust the roughness penalty to illustrate the underfit and overfit. . . . .	3
S-2	As in Figure 2, but all observations made in the stratosphere have been removed. . . . .	4
S-3	As in Figure 4, but all observations made in the stratosphere have been removed. . . . .	5
S-4	As in Figure 5, but all observations made in the stratosphere have been removed. . . . .	6
S-5	Monthly mean ozone time series and model fitted values on 4 upper-level layers above NE China. . . . .	7
S-6	Monthly mean ozone time series and model fitted values on 4 lower-level layers above NE China. . . . .	8
S-7	(a) Interannual component for the ozone distribution and (b) trend estimates and associated 2-sigma variabilities at 20 hPa vertical resolution, based on the separated fit and integrated fit methods above Trinidad Head, California. . . . .	9
S-8	(a) Interannual component for stratospheric ozone observation and (b) trend estimates and associated 2-sigma variabilities at 0.5 km vertical resolution, based on the separated fit and integrated fit methods above Hilo, Hawaii. . . . .	10

**Table S-1:** Percentage of (A) randomly generated and (B) fixed frequency sampled trends that fall outside of the 1- or 2- $\sigma$  intervals of the trend values that were derived from the full IAGOS data set. One thousand randomly generated trends were calculated on 15 pressure surfaces for each of a pre-determined scenario. Also shown are the associated mean absolute percentage error values.

(A) Number of profile-a-month		30	15	10	7	6	5	4	-	-	3
Separated fit	1- $\sigma$ range [%]	0.5	6.7	14.5	23.8	26.8	32.1	35.5	-	-	41.4
	2- $\sigma$ range [%]	0.0	0.0	0.4	2.0	3.1	4.5	7.0	-	-	10.6
	Error [%]	3.1	5.0	6.2	7.7	8.2	9.1	10.0	-	-	11.2
Integrated fit	1- $\sigma$ range [%]	0.3	4.2	10.3	18.8	21.6	26.0	30.0	-	-	36.0
	2- $\sigma$ range [%]	0.0	0.0	0.2	1.3	1.7	2.4	4.6	-	-	6.9
	Error [%]	2.7	4.4	5.5	6.8	7.3	8.1	8.8	-	-	9.9
(B) Sampling frequency [day]		1	2	3	4	5	6	7	8	9	10
Separated fit	1- $\sigma$ range [%]	0.5	5.1	10.9	17.9	23.9	27.4	32.0	35.3	37.0	41.2
	2- $\sigma$ range [%]	0.0	0.0	0.2	1.1	2.6	3.7	5.5	6.8	7.6	10.8
	Error [%]	3.1	4.5	5.6	6.7	7.8	8.3	9.1	9.7	10.1	11.1
Integrated fit	1- $\sigma$ range [%]	0.3	3.2	7.3	12.2	17.8	20.8	26.8	29.0	30.8	33.2
	2- $\sigma$ range [%]	0.0	0.0	0.1	0.5	1.6	1.9	3.2	4.1	4.4	6.3
	Error [%]	2.7	4.0	4.8	5.7	6.6	6.9	7.9	8.4	8.7	9.4

**Table S-2:** Trends and 2-sigma variabilities [in units of ppb decade<sup>-1</sup>] based on the separated fit and integrated fit methods, with a reference to different starting year, above Hilo, Hawaii and Trinidad Head (THD), California.

		Separated fit			Integrated fit		
		Trend	2-sigma	p-value	Trend	2-sigma	p-value
Hilo Since 1982	700-300hPa	1.11	0.83	0.01	1.12	0.78	0.01
	950-250hPa	0.89	0.68	0.01	0.96	0.63	<0.01
	950-800hPa	-0.25	0.70	0.47	0.02	0.56	0.95
	400-300hPa	2.31	1.10	<0.01	1.87	1.03	<0.01
	650hPa	0.21	0.86	0.63	0.70	0.67	0.05
Hilo Since 1994	700-300hPa	0.70	1.43	0.34	0.64	1.33	0.35
	950-250hPa	0.63	1.11	0.27	0.59	1.07	0.29
	950-800hPa	0.29	0.98	0.56	0.30	0.92	0.52
	400-300hPa	1.11	1.73	0.21	0.98	1.61	0.24
	650hPa	-0.05	1.34	0.94	-0.03	1.22	0.96
Hilo Since 2000	700-300hPa	0.07	2.01	0.95	0.04	1.83	0.96
	950-250hPa	0.02	1.50	0.98	-0.03	1.41	0.97
	950-800hPa	0.07	1.12	0.91	0.09	1.11	0.87
	400-300hPa	0.19	2.49	0.88	-0.19	2.17	0.86
	650hPa	-0.45	2.01	0.66	-0.09	1.64	0.91
		Separated fit			Integrated fit		
		Trend	2-sigma	p-value	Trend	2-sigma	p-value
THD Since 1998	700-300hPa	-2.46	2.45	0.06	-2.45	2.19	0.04
	950-250hPa	-1.85	1.70	0.04	-1.85	1.53	0.03
	950-800hPa	-0.81	0.90	0.09	-0.82	0.79	0.05
	400-300hPa	-5.65	5.73	0.06	-5.46	5.02	0.04
	650hPa	-0.48	1.46	0.52	-0.71	1.05	0.19
THD Since 2000	700-300hPa	-0.12	1.76	0.90	-0.22	1.47	0.76
	950-250hPa	-0.25	1.28	0.70	-0.33	1.09	0.55
	950-800hPa	-0.47	1.05	0.38	-0.52	0.92	0.28
	400-300hPa	-0.19	3.90	0.93	-0.32	3.04	0.84
	650hPa	-0.32	1.72	0.71	-0.41	1.19	0.50

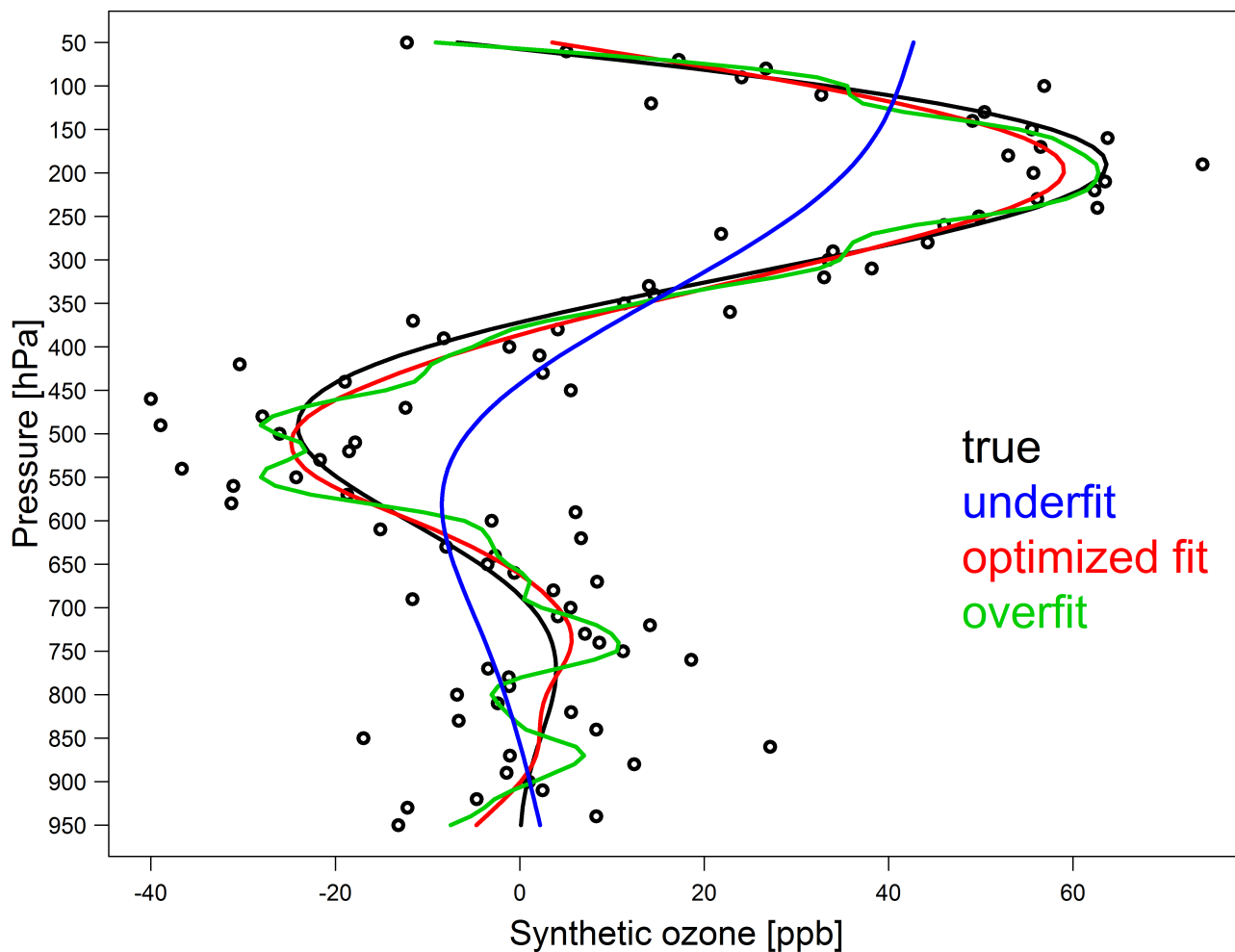
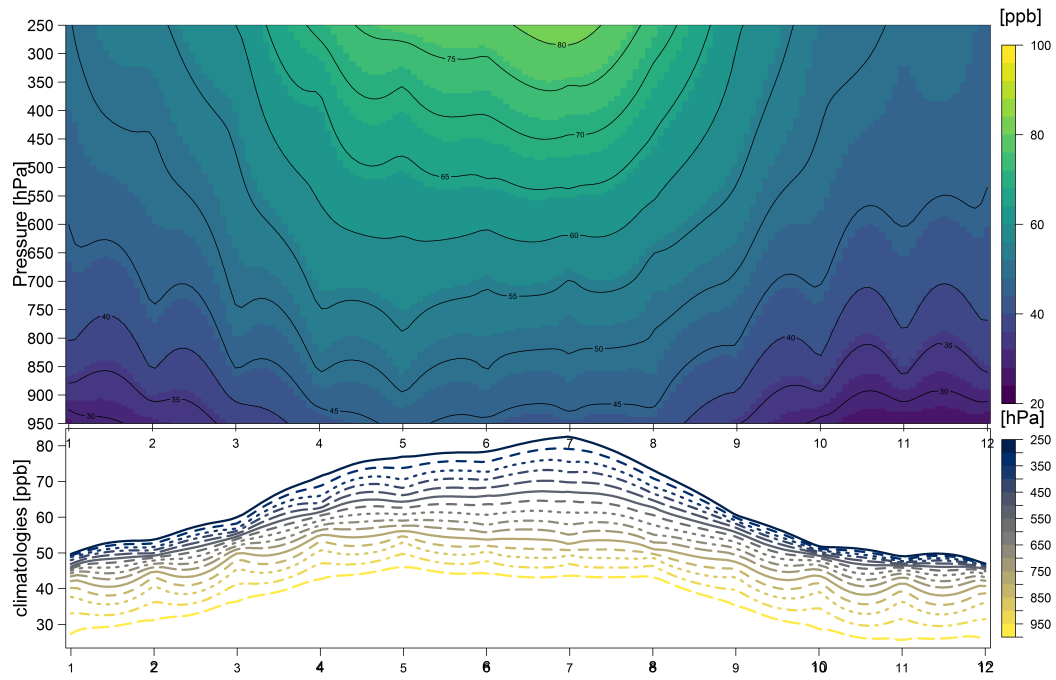
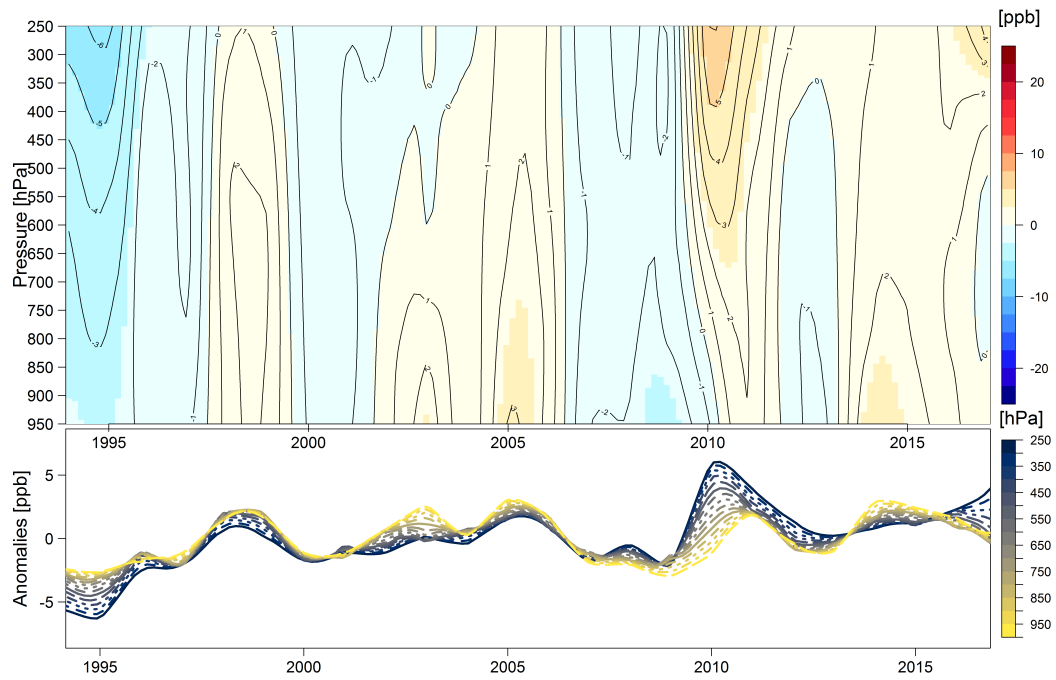


**Figure S-1:** A synthetic profile for the illustration of the issue of underfitting and overfitting. Data points are generated by adding random error to the function  $x = \sin(y/100) \times (y/100)^2$  (black curve). The appropriate fit should closely follow the true process (red curve), while the underfit indicates that the result failed to represent the general pattern of the true process (blue curve), and the overfit indicates that the result is overly complicated and is influenced by the noise component (green curve). Note that these three fits are based on the same model specification, except that we adjust the roughness penalty to illustrate the underfit and overfit.



(a) Seasonal component



(b) Interannual component

**Figure S-2:** As in Figure 2, but all observations made in the stratosphere have been removed.

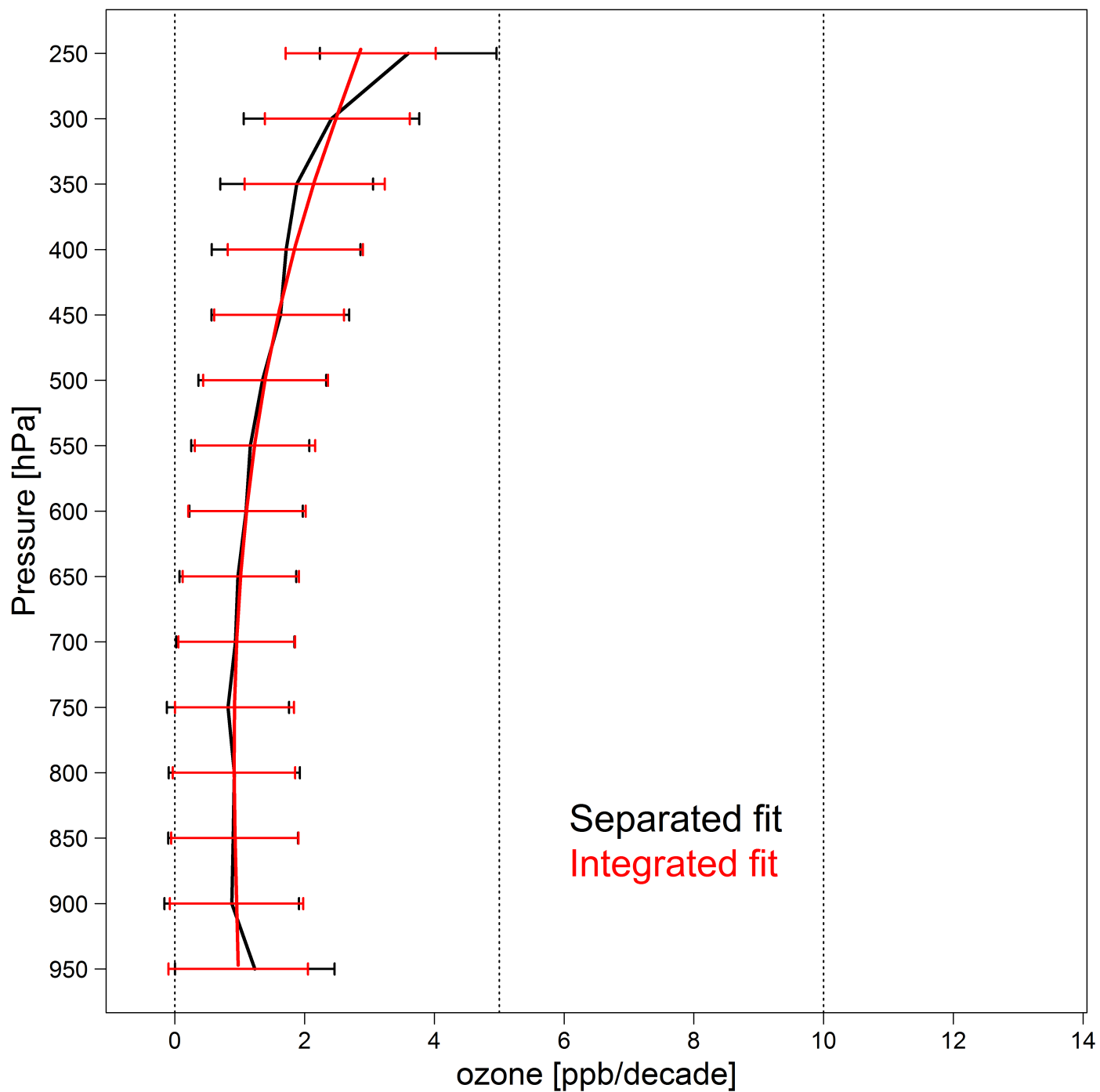


**Figure S-3:** As in Figure 4, but all observations made in the stratosphere have been removed.

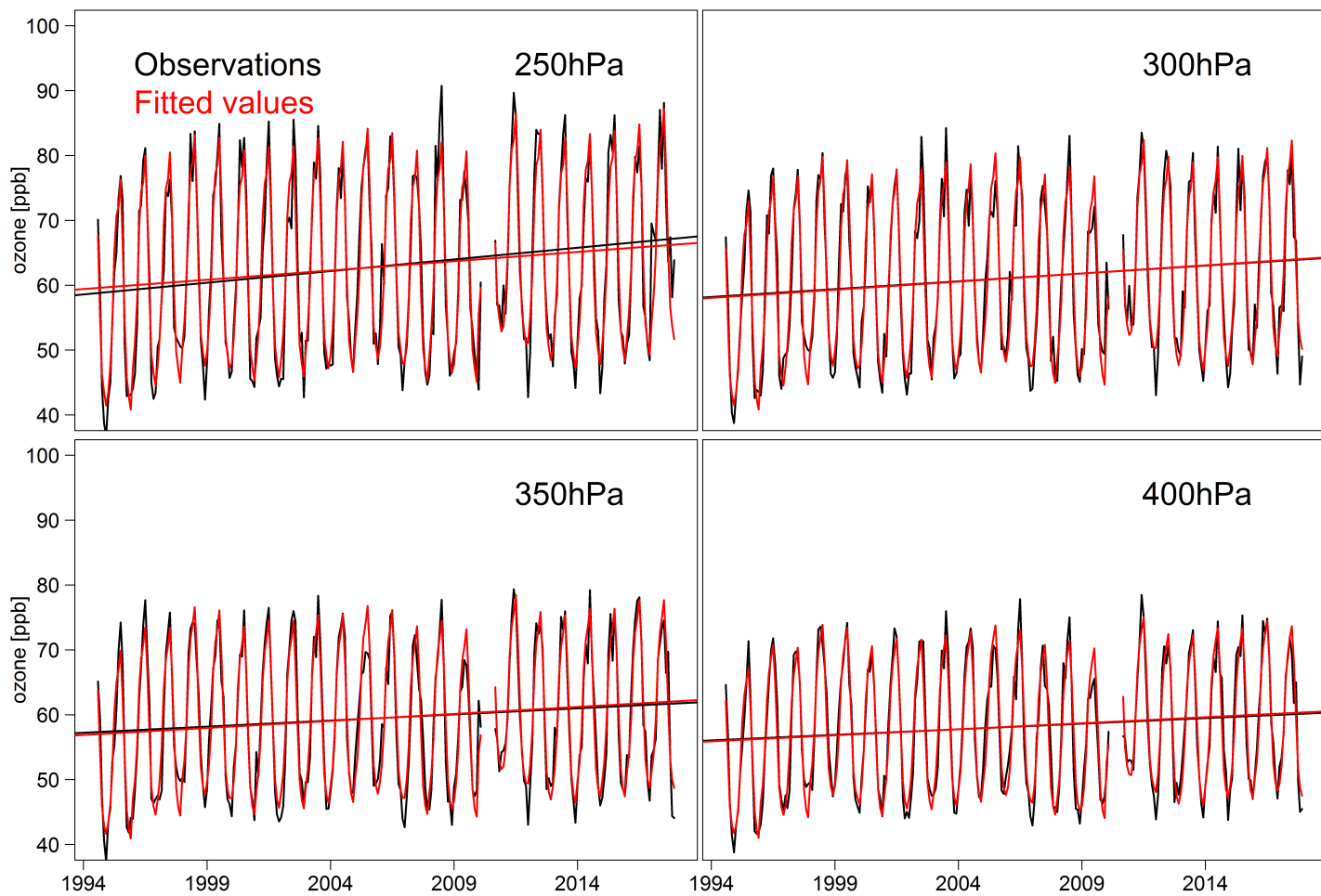


**Figure S-4:** As in Figure 5, but all observations made in the stratosphere have been removed.

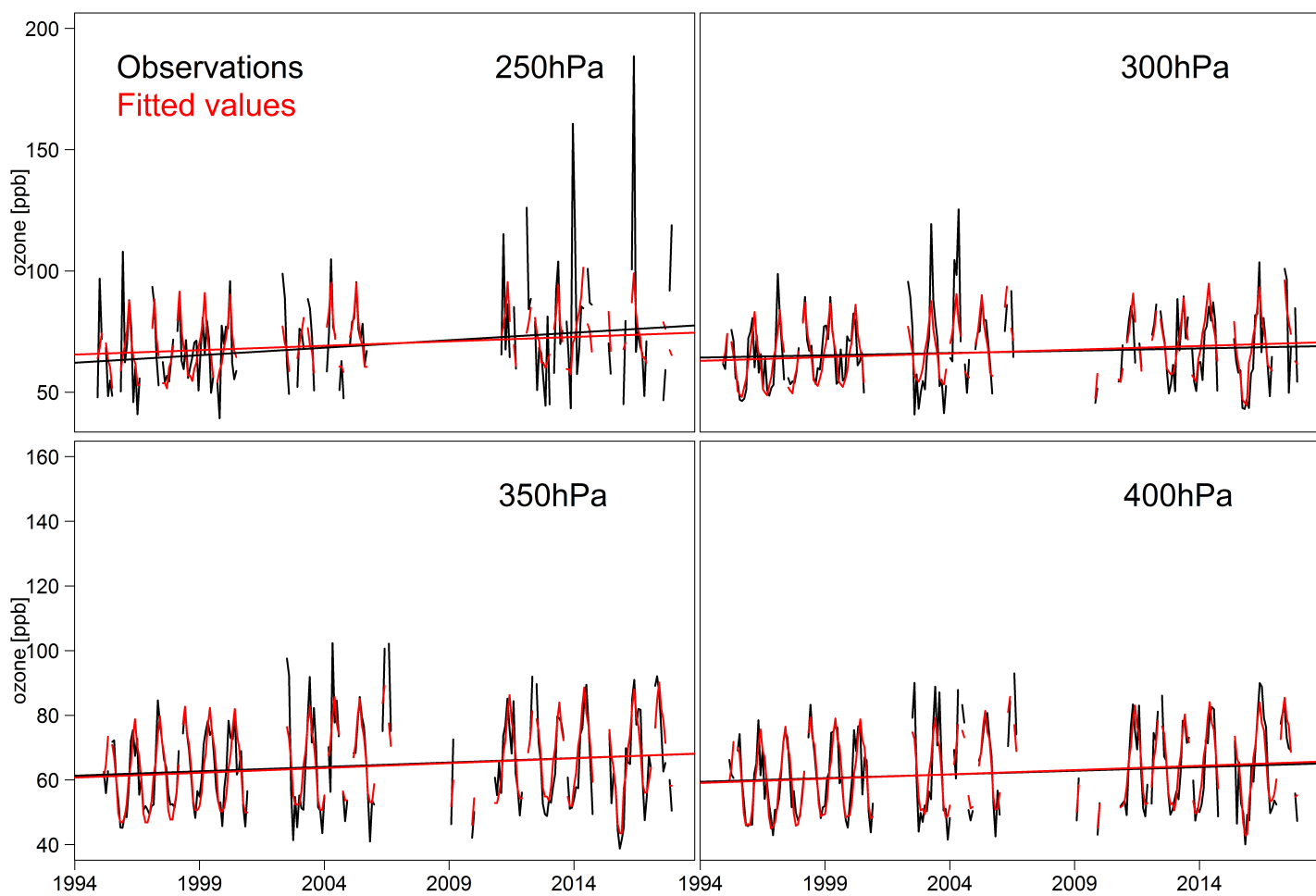


**Figure S-5:** Monthly mean ozone time series and model fitted values on 4 upper-level layers above NE China.



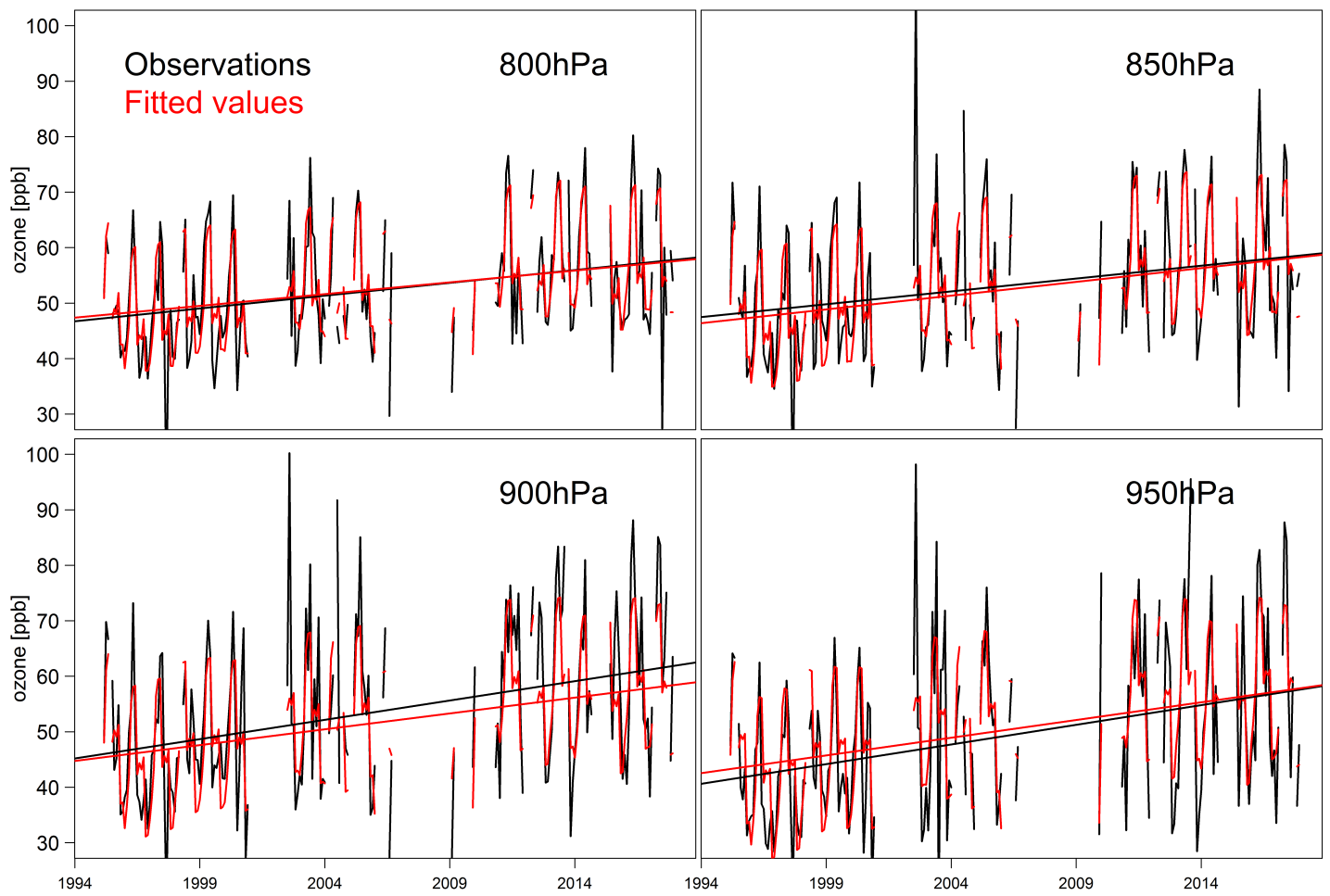
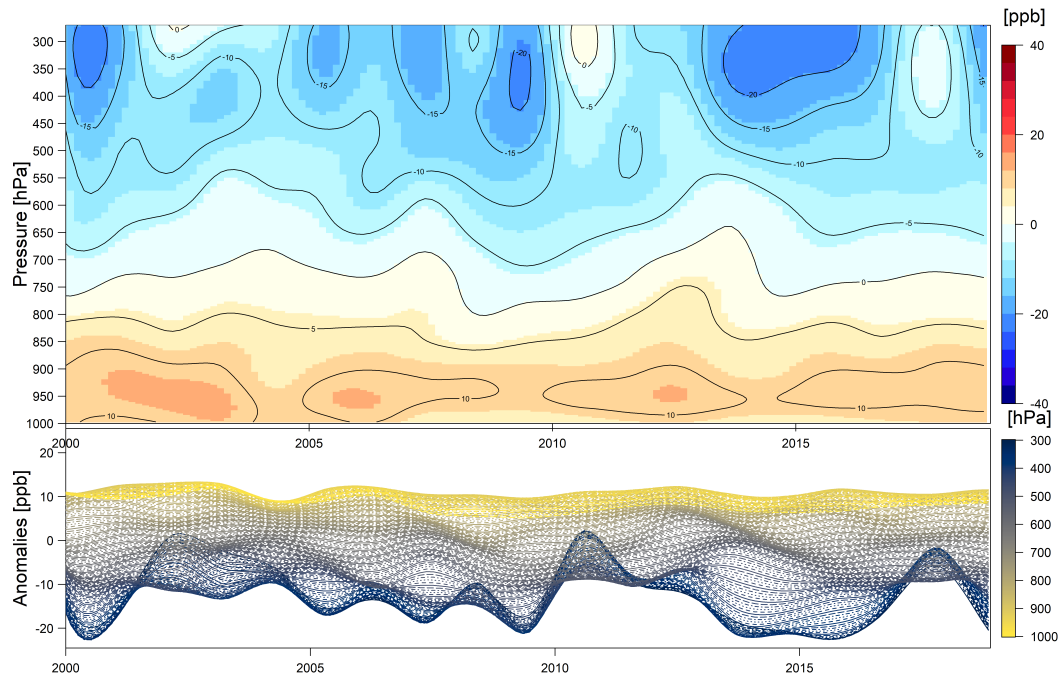
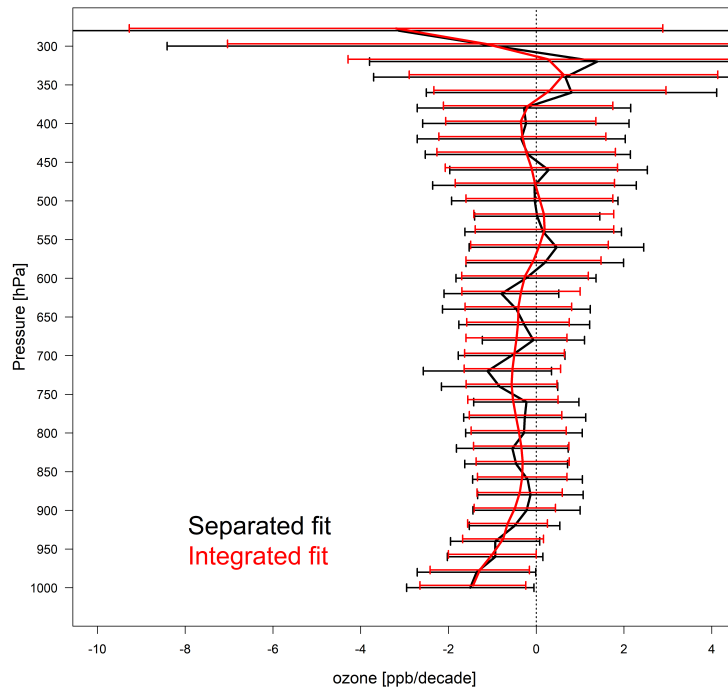


**Figure S-6:** Monthly mean ozone time series and model fitted values on 4 lower-level layers above NE China.

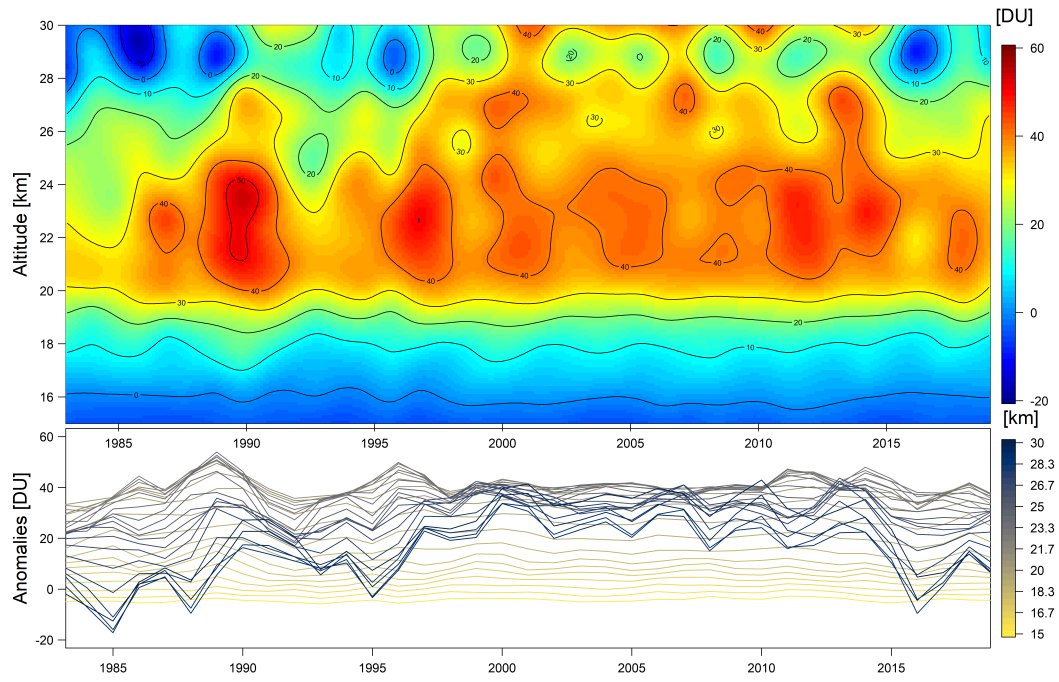


(a) Interannual component

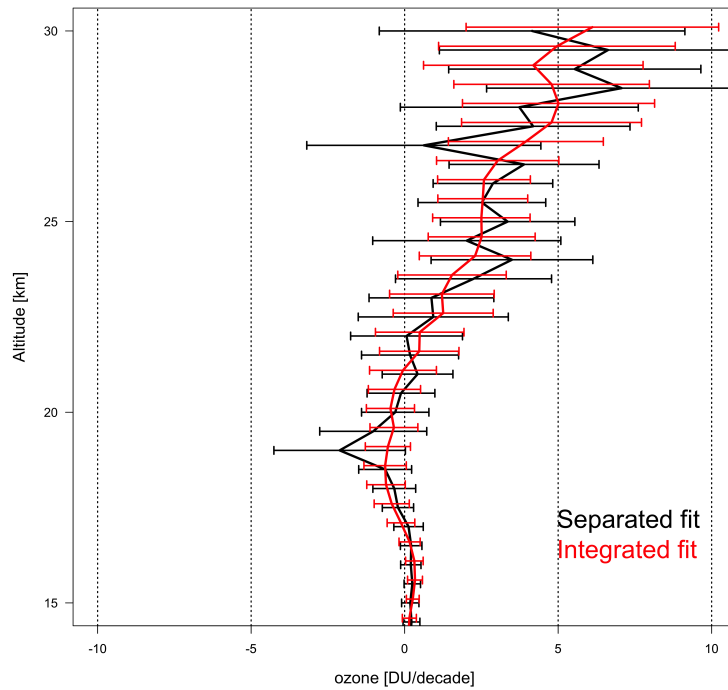


(b) Trend estimates (2000-2018)

**Figure S-7:** (a) Interannual component for the ozone distribution and (b) trend estimates and associated 2-sigma variabilities at 20 hPa vertical resolution, based on the separated fit and integrated fit methods above Trinidad Head, California.



(a) Interannual component



(b) Trend estimates (1982-2018)

**Figure S-8:** (a) Interannual component for stratospheric ozone observation and (b) trend estimates and associated 2-sigma variabilities at 0.5 km vertical resolution, based on the separated fit and integrated fit methods above Hilo, Hawaii.